Proceedings of Coastal and Ocean Engineering in Korea (2000)
Vol. 11, pp. 103-112

Derivation of Nonlinear Mild-Slope Equation and Numerical Simulation
비선형 완경사 방정식의 유도 및 수치모의

Jung Lyul Lee[1] and Chan Sung Park[2]
이정렬[1] · 박찬성[2]

1. INTRODUCTION

Early efforts to model wave transformation from offshore to inshore were based on the ray theory which accounts for wave refraction due to changes in bathymetry and the diffraction effects were ignored. Prediction of nearshore waves with the combined effects of refraction and diffraction as well as reflection has taken a new dimension with the use of the mild-slope equation and the Boussinesq equation. These two approaches in predicting nonlinear waves are essentially different in the sense that one is based on the linear wave characteristics and the other was started as an extensive work of the nonlinear shallow water waves.

1.1 Mild-Slope Equation Type

The mild-slope equation developed by Berkhoff (1972) has not only been used in its original form of an elliptic equation but also provided the basic governing equation for the development of other wave equations such as the parabolic equation (Radder, 1979), hyperbolic equation (Smith and Sprinks, 1975; Copeland, 1985; Madsen and Larsen, 1987), and elliptic equation of phase averaged type (Ebersole et al., 1986).

Chamberlain and Porter (1995) proposed a modified mild slope equation that includes the higher-order bottom effect terms as well as the evanescent modes. As an effort towards modeling the propagation of nonlinear waves, recently several time-dependent mild slope equations have also been developed by Lee (1994a), Nadaoka et al. (1994), and Isobe (1994).

1.1.1 Modified Mild Slope Equation

The modified mild-slope equation (Chamberlain and Porter, 1995) can be written as

$$\nabla\left(CCg\cdot\nabla\hat{\phi}\right)+k^2CCg\left(1+R\right)\hat{\phi}=0 \qquad (1)$$

where C and Cg are the local phase speed and the group velocity, respectively, g the gravitational acceleration, k the wave number, and $\hat{\phi}(x,y)$ the velocity potential at the mean water level. Equation (1) coincides with the familiar mild-slope equation if the term R is omitted. The retention of R widens the scope of Eq. (1), which is referred to as the modified mild-slope equation. The most simplified expression of R is given by Chamberlain and Porter(1995) as

[1] 성균관대학교 토목환경공학과 (Dept. of Civil and Environmental Eng., Sungkyunkwan University, Suwon Campus, Suwon 440-746, Korea)
[2] ㈜도화종합기술공사 항만부(Dept. of Port and Coast Eng., Dohwa Consulting Engineers Co., Ltd., Seoul 425-600, Korea)

$$R(h) = \frac{R_1}{k}\nabla^2 h + R_2\left(\nabla h\right)^2 \quad (2)$$

where

$$R_1 = \frac{\operatorname{csch}kh\operatorname{sech}kh}{4n(2kh+\sinh 2kh)}(\sinh 2kh - 2kh\cosh 2kh)$$

$$R_2 = \frac{\operatorname{csch}kh\operatorname{sech}kh}{12n(2kh+\sinh 2kh)}$$

$$[(2kh)^4 + 4(2kh)^3\sinh 2kh - 9\sinh 2kh\sinh 4kh$$

$$+6kh(2kh+2\sinh 2kh)(\cosh^2 2kh - 2\cosh 2kh + 3)]$$

Here n is the ratio of the group velocity Cg to the phase speed C, and the R_1 and R_2 are the dimensionless functions representing the effects of the bottom curvature and of the square of bottom slope, respectively. It is notable that R_2 approaches to $-1/6$ in the extremely shallow water.

1.1.2 Nonlinear Version

Lee's Equation

Lee (1994a) presented an equation set of nonlinear model for regular waves which can be applied to waves traveling from deep to shallow water.

$$\frac{\partial\eta}{\partial t} + \frac{1}{n}\nabla\cdot\left(\frac{nC^2}{g}\mathbf{u}\right) = 0 \quad (3)$$

$$\frac{\partial\mathbf{u}}{\partial t} + \frac{1}{2}\nabla(\mathbf{u}\cdot\mathbf{u}) + \frac{1}{2}\nabla\left(\frac{\partial\eta}{\partial t}\right)^2 + g\nabla\eta = 0 \quad (4)$$

where η is the free surface displacement, $\mathbf{u}$ the horizontal velocity vector defined at the free surface level, n the ratio of the group velocity Cg to the phase speed C, and as the dispersion relationship $\sigma^2 = gk\tanh kh$ is employed. The above equations completely satisfy the linear dispersion relationship and when expanded, they were proven to be consistent with Boussinesq equation of several types; Peregrine (1967), Madsen et al. (1991), and Nwogu (1993). In addition, the position of averaged velocity below the still water level was estimated based on the linear wave theory. For irregular waves, the following equation expressed in the alternative form of Smith and Sprinks (1975) instead of Eq. (3) is suggested.

$$\frac{\partial^2\eta}{\partial t^2} + \nabla\left(\frac{CCg}{g}\frac{\partial\mathbf{u}}{\partial t}\right) + \left(\sigma^2 - k^2CCg\right)\eta = 0 \quad (5)$$

Nadaoka's Equation

Nadaoka et al. (1994) derived a time-dependent nonlinear dispersive wave equation with the multi-term coupling technique, which are here given in the single-term representation as

$$\frac{\partial\eta}{\partial t} + \nabla\cdot\left[\left(\frac{C^2}{g} + \eta\right)\mathbf{u}_o\right] = 0 \quad (6)$$

$$CCg\frac{\partial\mathbf{u}_o}{\partial t} + C^2\nabla\left[g\eta + \eta\frac{\partial w_o}{\partial t} + \frac{1}{2}(\mathbf{u}_o\cdot\mathbf{u}_o + w_o^2)\right] = \frac{\partial}{\partial t}\left[\frac{C(C-Cg)}{k^2}\nabla(\nabla\cdot\mathbf{u}_o) + \nabla\left\{\frac{C(C-Cg)}{k^2}\right\}(\nabla\cdot\mathbf{u}_o)\right] \quad (7)$$

where $\mathbf{u}_o(u,v)$ is the two-dimensional horizontal velocity vector and w_o the vertical velocity. The subscript 'o' denotes the value defined at the mean water level. The vertical velocity, w_o was given as

$$w_o = -\nabla\cdot\frac{\tanh kh}{k}\mathbf{u}_o \quad (8)$$

The C, Cg, and k are respectively the phase and the group velocity, and the wave number which are obtained by the linear dispersion relationship under the prescribed incident frequency σ and local depth h.

Isobe's Equation

Isobe (1994) also derived nonlinear mild-slope equation as given below by expanding the velocity potential into a series in terms of a given set of vertical distribution functions and hence include full nonlinearity and full dispersivity.

$$f_\alpha^\eta\frac{\partial\eta}{\partial t} + \nabla\left(A_{\alpha\beta}\nabla\hat{\phi}_\beta\right) - B_{\alpha\beta}\hat{\phi}_\beta + \left(C_{\beta\alpha} - C_{\alpha\beta}\right)\left(\nabla\hat{\phi}_\beta\right)(\nabla h) + \frac{\partial f_\beta^\eta}{\partial h}f_\alpha^\eta\hat{\phi}_\beta(\nabla\eta)(\nabla h) = 0 \quad (9)$$

$$g\eta + f_\beta^\eta\frac{\partial\hat{\phi}_\beta}{\partial t} + \frac{1}{2}f_\gamma^\eta f_\beta^\eta\left(\nabla\hat{\phi}_\gamma\right)\left(\nabla\hat{\phi}_\beta\right) + \frac{1}{2}\frac{\partial f_\gamma^\eta}{\partial z}\frac{\partial f_\beta^\eta}{\partial z}\hat{\phi}_\gamma\hat{\phi}_\beta + \frac{\partial f_\gamma^\eta}{\partial h}f_\beta^\eta\hat{\phi}_\gamma\left(\nabla\hat{\phi}_\beta\right)(\nabla h) = 0 \quad (10)$$

where

$$f_\alpha^\eta = f_\alpha\big|_{z=\eta}, \quad \frac{\partial f_\alpha^\eta}{\partial z} = \frac{\partial f_\alpha}{\partial z}\bigg|_{z=\eta}$$

$$A_{\alpha\beta} = \int_{-h}^{\eta} f_\alpha f_\beta dz, \ B_{\alpha\beta} = \int_{-h}^{\eta} \frac{\partial f_\alpha}{\partial z}\frac{\partial f_\beta}{\partial z} dz, \ C_{\alpha\beta} = \int_{-h}^{\eta} \frac{\partial f_\alpha}{\partial h} f_\beta dz$$

The unknowns are η and $\hat{\phi}_\alpha$ (α =1 to N). The vertical distribution of the velocity potential, ϕ, is expressed as a series in terms of a set of vertical distribution functions, f_α :

$$\phi(\mathbf{x},z,t) = \sum_{\alpha=1}^{N} \hat{\phi}_\alpha(\mathbf{x},t) f_\alpha(z;h(\mathbf{x})) \equiv \hat{\phi}_\alpha f_\alpha \quad (11)$$

where $\hat{\phi}_\alpha$ is the coefficient to f_α and therefore independent of z, and $\mathbf{x} = (x, y)$ denotes the position vector on the horizontal plane. The f_α is expressed in the terms of the local water depth $h(\mathbf{x})$ as is normally the case. It was also shown that nonlinear shallow water equations and Boussinesq equations as well as mild-slope equation can be derived as special cases of the nonlinear mild-slope equations.

As the most simple case, Eqs. (9) and (10) can be expressed by the single component as follows.

$$f^\eta \frac{\partial \eta}{\partial t} + \nabla\left(A\nabla\hat{\phi}\right) - B\hat{\phi} = 0 \quad (12)$$

$$g\eta + f^\eta \frac{\partial \hat{\phi}}{\partial t} + \frac{1}{2}\left(f^\eta \nabla\hat{\phi}\right)^2 + \frac{1}{2}\left(\frac{\partial f^\eta}{\partial z}\hat{\phi}\right)^2 = 0 \quad (13)$$

If we assume $f(z) = \cosh k(h+z)/\cosh kh$ and $A = CCg/g$ and $B = (\sigma^2 - k^2 CCg)/g$. Assuming $f^\eta = 1$, we obtain

$$\frac{\partial \eta}{\partial t} + \nabla\left(\frac{CCg}{g}\nabla\hat{\phi}\right) - \frac{\sigma^2 - k^2 CCg}{g}\hat{\phi} = 0 \quad (14)$$

$$\frac{\partial \hat{\phi}}{\partial t} + g\eta + \frac{1}{2}\left(\nabla\hat{\phi}\right)^2 + \frac{1}{2}\hat{w}^2 = 0 \quad (15)$$

Therefore, the above can be consistent with Lee (1994)'s equation in single component expression.

1.2 Boussinesq Equation Type

The classical Boussinesq equations for one-dimensional propagation were first presented by Boussinesq(1872, 1877) and later the equations were extended to two-dimensional propagation over mildly sloping bottoms by Peregrine(1967). The Boussinesq type equations are known to simulate the combined effects of nonlinear short wave phenomena in shallow water areas quite well. Their major restriction, however, is to incorporate only weak dispersion and weak nonlinearity. Generally, the weak dispersion is more critical restriction as it directly affects the accuracy of both wave celerity and group velocity which is crucial for most wave dynamics. This problem has attracted considerable attention in the last 10 years. Numerous other formulations, therefore, have been developed to improve dispersion characteristics.

2. NONLINEAR VERSION OF MILD-SLOPE EQUATION

2.1 Derivation

The nonlinear mild-slope equation will be derived directly from the continuity equations by using the Galerkin's method. The continuity equations of an incompressible fluid are given by

$$\nabla \cdot \mathbf{u} + \frac{\partial w}{\partial z} = 0 \quad (16)$$

where $\mathbf{u}$, w are the horizontal velocity and vertical velocity components, respectively. A bold face symbol indicates two horizontal components of flow vector; $\mathbf{u} = (u, v)$. The two-dimensional gradient operator $(\partial/\partial x, \partial/\partial y)$, is denoted by ∇ . We multiply $f(z)$ to Eq. (16), and integrate from the bottom to the free surface.

$$\int_{-h}^{\eta} f\nabla \cdot u dz + \int_{-h}^{\eta} f\frac{\partial w}{\partial z} dz$$
$$= \int_{-h}^{\eta} \nabla \cdot (fu) dz - \int_{-h}^{\eta} u \cdot \nabla f dz - \int_{-h}^{\eta} \left(\frac{\partial f}{\partial z}\right)^2 dz\hat{\phi} \quad (17)$$
$$+ \int_{-h}^{\eta} \frac{\partial}{\partial z}(fw) dz = 0$$

where, η is the free surface displacement and $\mathbf{u}$ is given by $\nabla\phi$ in terms of velocity potential. For the slowly varying water depth, the wave part of the velocity potential may be written as

$$\phi(\mathbf{x},z,t) = f(z)\hat{\phi}(\mathbf{x},t) \quad (18)$$

where, $f(z)$ =cosh $k(h+z)$ /cosh kh is a slowly varying function of x and $\hat{\phi}$ denotes the velocity potential at the mean water level, termed as 'the surface potential'. Recall Leibnitz's rule

$$\nabla \cdot \int_{\beta}^{\alpha} f dz = \int_{\beta}^{\alpha} \nabla \cdot f dz + f|_{\beta} \nabla\beta - f|_{\alpha} \nabla\alpha$$

to obtain the following expression from Eq. (17).

$$\begin{aligned}&\nabla \cdot \int_{-h}^{\eta} f^2 dz \nabla\hat{\phi} - \int_{-h}^{\eta}\left(\frac{\partial f}{\partial z}\right)^2 dz\hat{\phi} - [\nabla\eta \cdot f\mathbf{u}]_{\eta} \\ &-[\nabla h \cdot f\mathbf{u}]_{-h} + [fw]_{\eta} - [fw]_{-h} = 0\end{aligned} \quad (19)$$

Taking Taylor expansion about $\eta = 0$ to Eq. (19),

$$\begin{aligned}&\nabla \cdot \int_{-h}^{0} f^2 dz \nabla\hat{\phi} - \int_{-h}^{0}\left(\frac{\partial f}{\partial z}\right)^2 dz\hat{\phi} + \nabla\cdot(\eta\nabla\hat{\phi}) - \frac{\sigma^4}{g^2}\eta\hat{\phi} \\ &-[\nabla\eta \cdot f\mathbf{u}]_{\eta} - [\nabla h \cdot f\mathbf{u}]_{-h} + [fw]_{\eta} - [fw]_{-h} = 0\end{aligned} \quad (20)$$

where

$$\int_{-h}^{0} f^2 dz = \frac{CCg}{g}$$

$$\int_{-h}^{0}\left(\frac{\partial f}{\partial z}\right)^2 dz = \frac{\sigma^2 - k^2 CCg}{g}$$

Substituting the kinematic boundary conditions at free surface($z = \eta$) and at bottom($z = -h$) into Eq. (20),

$$w|_{\eta} - \frac{\partial\eta}{\partial t} - \mathbf{u}_{\eta} \cdot \nabla\eta = 0 \quad (21)$$

$$w|_{-h} + \mathbf{u}_{-h} \cdot \nabla h = 0 \quad (22)$$

and obtain following equation:

$$\begin{aligned}&\frac{\partial\eta}{\partial t} + \nabla \cdot \left[\left(\frac{CCg}{g} + \eta\right) u_0\right] \\ &-\frac{\sigma^2 - k^2 CCg}{g}\hat{\phi} - \frac{\sigma^4}{g^2}\eta\hat{\phi} = 0\end{aligned} \quad (23)$$

Differentiating by the variable t:

$$\begin{aligned}&\frac{\partial^2\eta}{\partial t^2} + \nabla \cdot \left[\left(\frac{CCg}{g} + \eta\right)\left(\frac{\partial\mathbf{u}_o}{\partial t}\right)\right] + \nabla \cdot \left(\mathbf{u}_o \frac{\partial\eta}{\partial t}\right) \\ &-\frac{\sigma^2 - k^2 CCg}{g}\frac{\partial\hat{\phi}}{\partial t} - \frac{\sigma^4}{g^2}\frac{\partial(\eta\hat{\phi})}{\partial t} = 0\end{aligned} \quad (24)$$

where C , Cg , σ and k are assumed to be time independent. Substituting the dynamic free surface boundary condition,

$$\frac{\partial\hat{\phi}}{\partial t} + \frac{1}{2}\left(\mathbf{u}_o{}^2 + w_o{}^2\right) + g\eta + \eta\frac{\partial w_o}{\partial t} = 0 \quad (25)$$

and assuming the last terms in Eq. (24) and (25),

$$\frac{\partial(\eta\hat{\phi})}{\partial t} \approx -2g\eta^2 \quad (26)$$

$$\eta\frac{\partial w_o}{\partial t} \approx \left(\frac{\partial\eta}{\partial t}\right)^2 \quad (27)$$

respectively and then yield following equation:

$$\begin{aligned}&\frac{\partial^2\eta}{\partial t^2} + \nabla \cdot \left[\left(\frac{CCg}{g} + \eta\right)\left(\frac{\partial\mathbf{u}_o}{\partial t}\right)\right] + \nabla \cdot \left(\mathbf{u}_o \frac{\partial\eta}{\partial t}\right) \\ &+\frac{\sigma^2 - k^2 CCg}{g}\left[\frac{1}{2}\mathbf{u}_o^2 + g\eta + \frac{3}{2}\left(\frac{\partial\eta}{\partial t}\right)^2\right] + 2\frac{\sigma^4}{g}\eta^2 = 0\end{aligned} \quad (28)$$

The above equation is combined with the nonlinear momentum equation defined at the free surface.

$$\frac{\partial\mathbf{u}_{\eta}}{\partial t} + \nabla\left[g\eta + \int_z^{\eta}\frac{\partial w}{\partial t}dz + \frac{1}{2}\left(\mathbf{u}_{\eta} \cdot \mathbf{u}_{\eta} + w_{\eta}{}^2\right)\right] = 0 \quad (29)$$

Taking Taylor expansion about $\eta = 0$,

$$\frac{\partial\mathbf{u}_o}{\partial t} + \nabla\left[g\eta + \eta\frac{\partial w_o}{\partial t} + \frac{1}{2}\left(\mathbf{u}_o \cdot \mathbf{u}_o + w_o{}^2\right)\right] = 0 \quad (30)$$

and assuming

$$w_o^2 = \left(\frac{\partial\eta}{\partial t}\right)^2 \quad (31)$$

shown in the nonlinear term and then finally we obtain the following momentum equation:

$$\frac{\partial \mathbf{u}_o}{\partial t} + g\nabla\eta + \mathbf{u}_o \cdot \nabla \mathbf{u}_o + \frac{3}{2}\nabla\left(\frac{\partial \eta}{\partial t}\right)^2 = 0 \quad (32)$$

Therefore, Eqs. (28) and (32) are a set of the governing equations used for nonlinear wave propagation in this study. We used the Miche's criterion (Miche, 1951) because the breaking wave model is simple and accurate enough, and guarantees stability. For the mass conservation, the broken mass due to wave breaking is consequently passed on the next step elevation at each grid.

2.2 Single Component Model

Combining Eqs. (28) and (32), yields

$$\frac{\partial^2 \eta}{\partial t^2} - \nabla \cdot \left[\frac{CCg}{g}\nabla\left(g\eta + \frac{\mathbf{u}_o^2}{2} + \frac{3\sigma^2}{2}\eta^2\right)\right] + \nabla \cdot \left[\frac{\partial(\eta \mathbf{u}_o)}{\partial t}\right] + \left[\frac{\sigma^2 - k^2 CCg}{g}\right]\left[g\eta + \frac{\mathbf{u}_o^2}{2} + \frac{3\sigma^2}{2}\eta^2\right] + 2\frac{\sigma^4}{g}\eta^2 = 0 \quad (33)$$

In order to eliminate the velocity components except η, the following approximate relations are applied.

$$\mathbf{u}_o^{\,2} = \frac{g^2}{C^2}\eta^2, \quad \frac{\partial(\eta \mathbf{u}_o)}{\partial t} = -g\nabla\eta^2$$

Then we obtain

$$\frac{\partial^2 \eta}{\partial t^2} - \nabla \cdot \left[\frac{CCg}{g}\nabla\left(g\eta + \frac{g^2\eta^2}{2C^2} + \frac{3\sigma^2}{2}\eta^2\right)\right] - g\nabla^2\eta^2 + \left[\frac{\sigma^2 - k^2 CCg}{g}\right]\left[g\eta + \frac{g^2\eta^2}{2C^2} + \frac{3\sigma^2}{2}\eta^2\right] + 2\frac{\sigma^4}{g}\eta^2 = 0 \quad (34)$$

For the asymptotic analysis, the above is re-expressed as

$$\frac{\partial^2 \eta}{\partial t^2} = \nabla \cdot \left[\frac{CCg}{g}\nabla\left(g\eta + \frac{g^2\eta^2}{C^2}\left(\frac{1}{2} + \frac{3}{2}\tanh^2 kh\right)\right)\right] + g\nabla^2\eta^2 - \left[\frac{k^2C^2(1-n)}{g}\right]\left[g\eta + \frac{g^2\eta^2}{C^2}\left(\frac{1}{2} + \frac{3}{2}\tanh^2 kh\right)\right] - 2gk^2\tanh^2 kh\eta^2 \quad (35)$$

We shall now consider the special forms of Eq. (35) when depth is relatively shallow and deep. In the very shallow water so that $C = Cg = \sqrt{gh}$ and $\tanh^2 kh \simeq 0$, Eq. (35) becomes

$$\frac{\partial^2 \eta}{\partial t^2} = g\nabla \cdot (h\nabla\eta) + \frac{g}{2}\nabla \cdot \left(h\nabla\frac{\eta^2}{h}\right) + g\nabla^2\eta^2 \quad (36)$$

which may be shown to be the combined form of Airy(1845)'s non-dispersive nonlinear wave equations for varying depth, correct to the second-order in nonlinearity.

Next, the phase speed and the group velocity are given in lowest-order dispersion as

$$C = \sqrt{gh}\left(1 - k^2h^2/6\right) \text{ and } Cg = \sqrt{gh}\left(1 - k^2h^2/2\right)$$

Replacing them should result in the combined version of Boussinesq equation.

$$\frac{\partial^2 \eta}{\partial t^2} = \nabla \cdot \left[\frac{gh\left(1-\frac{k^2h^2}{6}\right)\left(1-\frac{k^2h^2}{2}\right)}{g}\nabla\left(g\eta + \frac{g^2\eta^2}{2gh\left(1-\frac{k^2h^2}{6}\right)^2}\right)\right] + g\nabla^2\eta^2$$
$$-\left[\frac{k^2gh\left(1-\frac{k^2h^2}{6}\right)^2 - k^2gh\left(1-\frac{k^2h^2}{2}\right)\left(1-\frac{k^2h^2}{6}\right)}{g}\right]\left[g\eta + \frac{g^2\eta^2}{2gh\left(1-\frac{k^2h^2}{6}\right)^2}\right]$$
$$\cong \nabla \cdot \left[h\left(1-\frac{2}{3}k^2h^2\right)\nabla\left(g\eta + \frac{g\eta^2}{2h(1-k^2h^2/3)}\right)\right] + g\nabla^2\eta^2$$
$$-k^2h\left(\frac{k^2h^2}{3}\right)\left[g\eta + \frac{g\eta^2}{2h(1-k^2h^2/3)}\right] \quad (37)$$

Retaining the leading order,

$$\frac{\partial^2 \eta}{\partial t^2} = g\nabla \cdot (h\nabla\eta) - \frac{2g}{3}\nabla \cdot \left(k^2h^3\nabla\eta\right) + \frac{g}{2}\nabla \cdot \left(h\nabla\frac{\eta^2}{h}\right) + g\nabla^2\eta^2 - \frac{k^4h^3}{3}g\eta \quad (38)$$

For the constant depth, invoking the relation $k^2\eta = -\nabla^2\eta$,

$$\frac{\partial^2 \eta}{\partial t^2} = g\nabla \cdot (h\nabla\eta) + \frac{1}{3}gh^3\nabla^2\left(\nabla^2\eta\right) + \frac{3g}{2}\nabla^2\eta^2 \quad (39)$$

which is in accordance with the classical Boussinesq approximations.

For the deep water of constant depth, $C = \sqrt{g/k}$ and $Cg = C/2$. In this case, Eq. (35) can be approximated as

$$\frac{\partial^2 \eta}{\partial t^2} = \frac{g}{k}\nabla^2\eta + \frac{11g}{4}\nabla^2\eta^2 \tag{40}$$

with $k^2\eta^2 \simeq -\nabla^2\eta^2/4$ based on the Stokes wave theory.

If Eq. (33) is linearized, the time-dependent mild-slope equation proposed by Smith and Sprinks (1975) is obtained as

$$\frac{\partial^2 \eta}{\partial t^2} - \nabla\cdot\left[CCg\nabla\eta\right] + \left[\sigma^2 - k^2 CCg\right]\eta = 0 \tag{41}$$

2.3 Numerical Analysis

The governing equations (28) and (32) are similar form to a set of the shallow water equations. They are solved here by using a fractional step method in conjunction with the approximate factorization techniques leading to the implicit finite difference schemes. Since the time step of an explicit scheme is limited by the Courant-Friedrichs-Lawy (CFL) condition, it is advisable to reduce the number of time steps by use of an implicit scheme. A fraction step method is based on the recognition that the physical phenomena of water flow are represented by superimposing individual operations as Chorin (1968) pointed out. Therefore, the momentum equations, which have the nonlinear advective term, are divided into the two elementary operations; advection and propagation, and solved by using a fractional step method.

3. PHYSICAL EXPERIMENTS

The experiment was conducted in a Coastal-Hydraulics Laboratory wave flume of Sungkyunkwan University, in order to verify the numerical results of nonlinear waves. The wave flume of 50 *cm* deep, 40 *cm* wide, and 12 *m* long consists of a wave generator and beach zones. The bottom and side walls of the flume are glass to allow easy optical access. The regular waves were generated by a piston-type wave paddle and the beach slope of 1/19 was set at the other end of the wave flume.

The wave flume was decorated with the data acquisition system accessing the wave profile signals from the wave gages. Gages were connected with amplifier for increasing analog signals. Then the DaqBoard 100A (DaqBoard), A/D converter, changes conditioned signals into corresponding digital numbers saved as ASCII format.

Physical experiments were accomplished for two cases. Experimental conditions consist of same wave conditions for two different experimental setup, respectively. Wave conditions for Case 1-A and Case 2-A are T=0.8sec, Hi= 2*cm*, Ur=10.05 and steepness= 0.0282. Wave conditions for Case 1-B and Case 2-B are T=1.0sec, Hi= 1.5*cm*, Ur=12.80 and steepness= 0.0162. The Ursell parameter is a dimensionless parameter that is useful to define the range of application of the various wave theories. Generally cnoidal theory is applicable for $Ur > 25$ and Stokes theory is applicable for $Ur < 10$.

The layouts of two different experimental configurations are illustrated in Figs. 1 and 2 with the locations of the measurement stations and detailed geometry of the flume. The exposed breakwater is placed to the left half of the wave tank looking in the direction of the wave propagation, while the submerged breakwater is placed to the left side.

As shown in Fig. 1, wave gages 1, 2 and 3 for Case 1 were located at x=41*cm*, x=81*cm* and x=121*cm* measured shoreward from the toe of slope, respectively. The measuring section was located about 10.5 *cm* apart from the nearer sidewall.

As for the submerged breakwater shown in Fig. 2. wave gages 1, 2 and 3 were located at x=-12.5*cm*, x=0*cm* (center) and x=21*cm* measured shoreward from the center of submerged breakwater, respectively. The squared submerged breakwater is impermeable and has 1.1 *cm* height and 15 *cm* length.

4. RESULTS

Figures 3 and 4 show a comparison between the observed and calculated temporal wave profiles for Case 1. The time series were synchronized with the computations at station 1. The measured results are also shown in each figure by closed circles. The agreement appears to be generally acceptable, though it is evident that both results show the weak irregularity. In Case 1-A, the waves measured at stations 2 and 3 show the strong asymmetry due to nonlinearity as we expected. While several peaks in a period are shown in Case 1-B experiments, differently from the numerical prediction. Judging from the detailed experiments using a moving cart, they seemed to be caused by reflection of asymmetric waves (radiating from a breakwater) rather than the wave decomposition. Such multi-peaks can occur under wave decomposition. The wave decomposition is usually caused by a nonlinear wave train passing over a submerged bar or a submerged shelf. In this case, however, there is no submerged shelf but a breakwater causes the strong reflection. Figures 5 and 6 show the 3-D perspective views of instantaneous water surface elevation for two different wave conditions obtained from the numerical model. In those figures, the wave diffraction is shown behind a breakwater.

Figures 7 and 8 give the comparison of temporal wave profiles for Case 2. The numerical results are in good agreement with those of the observed data. Figures 9 and 10 show the 3-D views of instantaneous water surface elevation for two different wave conditions obtained from the numerical model. It is shown in Figs. 9 and 10 that wave profiles are deformed over the submerged breakwater section. The submerged breakwater seems to cause neither the strong wave decomposition nor predominant multi-peaks because its height is relatively thin.

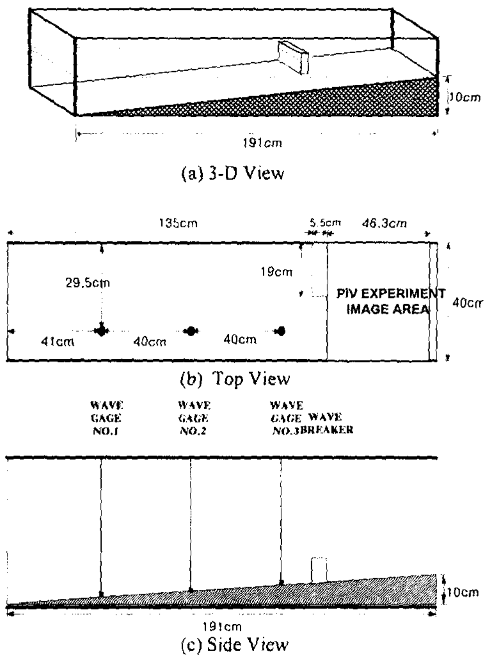

Figure 1. Physical layout of experiment Case 1: (a) 3-D view, (b) top view, (c) side view.

5. CONCLUSION

The nonlinear mild-slope equation was derived directly from the continuity equation by using the Galerkin's method. In modeling breaking waves we employed the Miche's criterion which believed to be simple, stable, and reliable.

We verified nonlinear wave model capacity through comparison of numerical simulation to physical experiments for two configurations; the exposed breakwater and the submerged breakwater. The overall agreement appeared for the exposed breakwater, though it is evident that the weak irregularity in experimental data measurements showed. The waves showed strong asymmetry due to nonlinearity and multi-peaks due to reflection of nonlinear waves. Such phenomena might increase with Ursell parameter increasing.

In the submerged breakwater, the best agreement was shown. Wave profiles appeared to be deformed due to a submerged breakwater. However, neither wave decomposition nor multi-peaks seems to be strongly observed in the case of the submerged breakwater because its height is relatively thin.

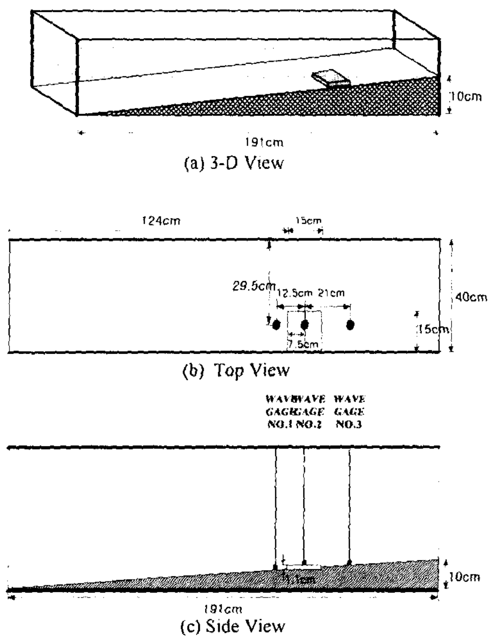

Figure 2. Physical layout of experiment Case 2: (a) 3-D view, (b) top view, (c) side view.

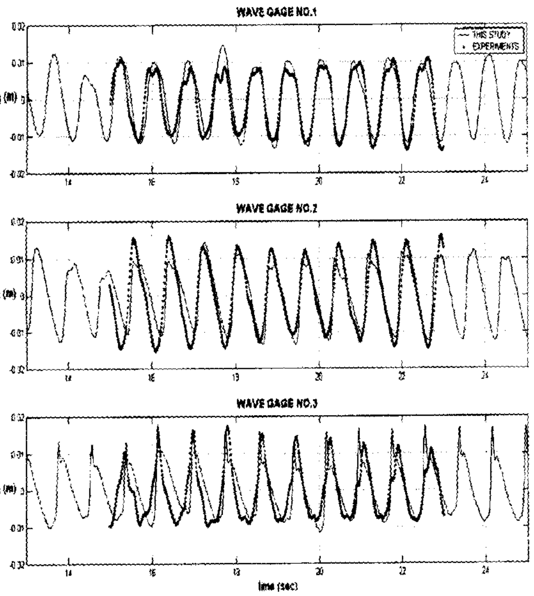

Figure 3. Comparison of wave profiles at wave gages No. 1, 2 and 3 of Case 1-A. (*Hi*=2.0 *cm*, *T*=0.8 *s*)

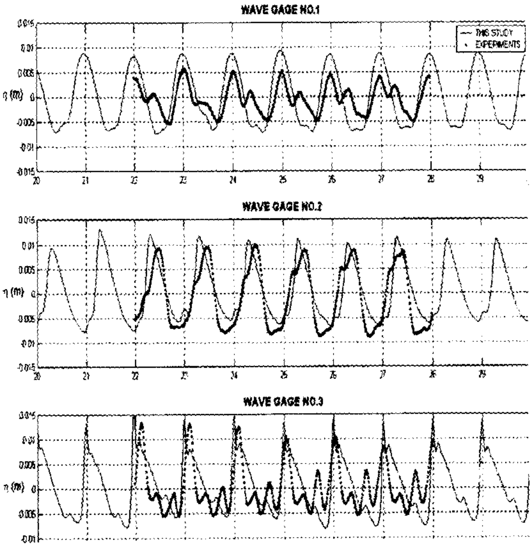

Figure 4. Comparison of wave profiles at wave gages No. 1, 2 and 3 of Case 1-B. (*Hi* =1.5 *cm*, *T*=1.0 *s*)

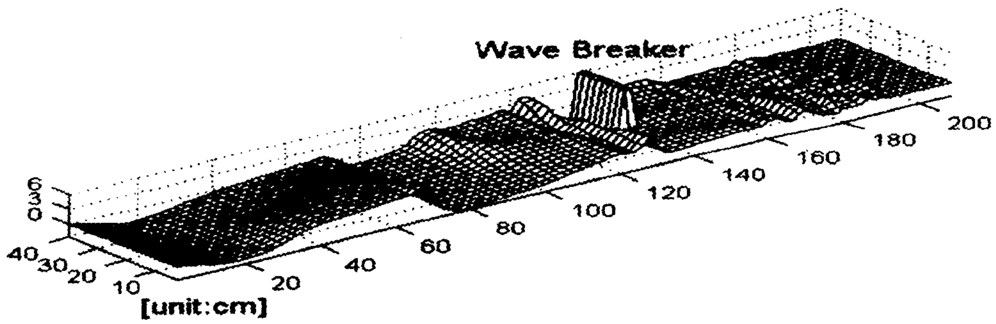

Figure 5. 3-D view of nonlinear wave propagation by numerical model for Case 1-A

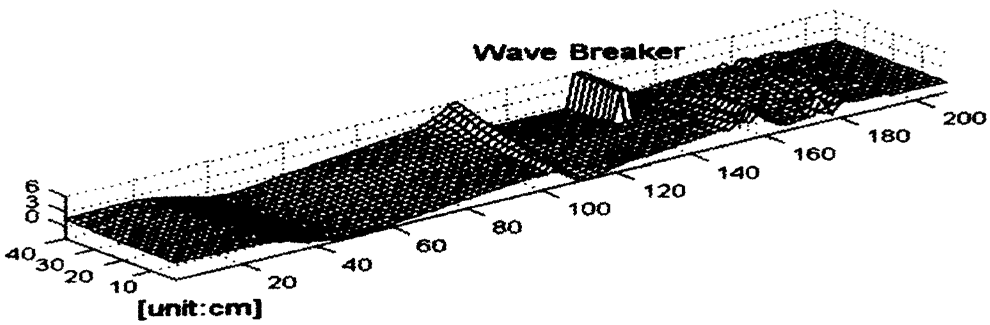

Figure 6. 3-D view of nonlinear wave propagation by numerical model for Case 1-B

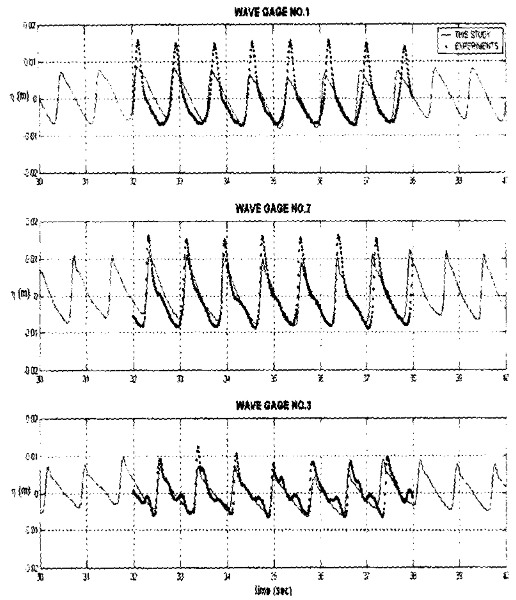

Figure 7. Comparison of wave profiles at wave gages No. 1, 2 and 3 of Case 2-A. (*Hi* =2.0 *cm*, *T*=0.8 *s*)

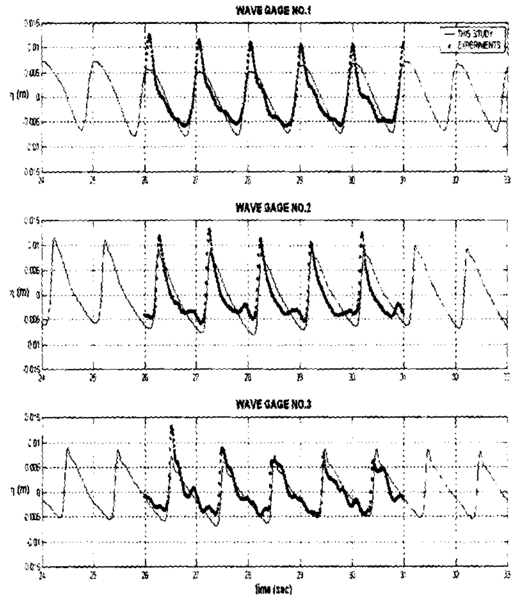

Figure 8. Comparison of wave profiles at wave gages No. 1, 2 and 3 of Case 2-B. (*Hi* =1.5 *cm*, *T*=1.0 *s*)

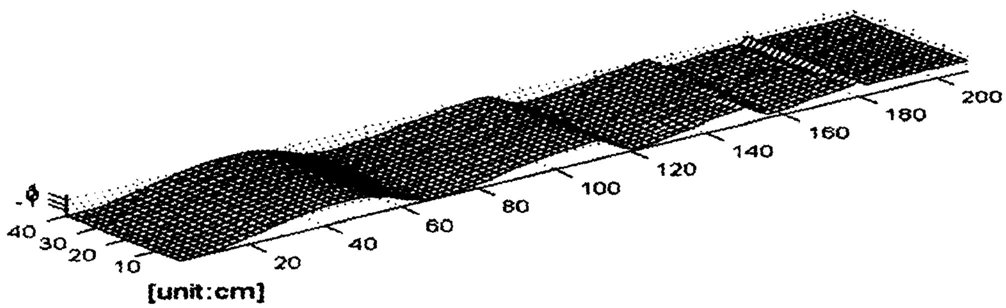

Figure 9. 3-D view of nonlinear wave propagation by numerical model for Case 2-A

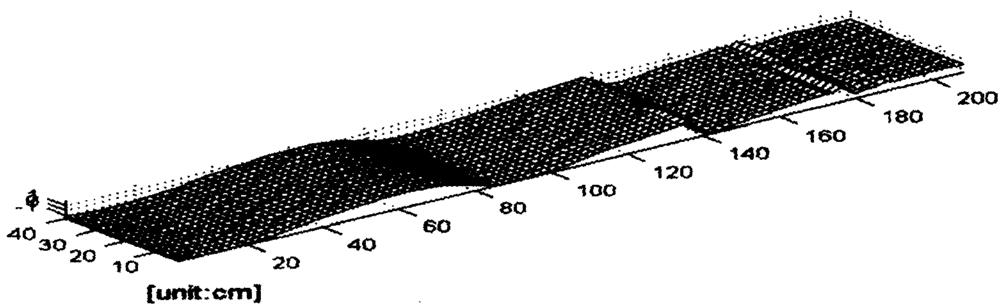

Figure 10. 3-D view of nonlinear wave propagation by numerical model for Case 2-B

ACKNOWLEDGMENTS

Funding for this research from Korea Science and Engineering Foundation(KOSEF 961-1204-017-1) is gratefully acknowledged.

REFERENCES

Airy, G.B., 1845. Tides and waves, Encyclopedia Metropolitana, Art. 192, London.

Berkhoff, J.C.W., 1972. Computation of combined refraction-diffraction, *Proc. 13rd Int. Conf. Coastal Engrg.*, ASCE, 471-490.

Boussinesq, J., 1872. Théorie des ondes et des remous qui se propagent le long d'un canal rectangulaire horizontalen communiquant au liquide continue dans cd canal des vitesse sensibliement pareilles de la surface du fond, *J. Math. Pure et Appliqué*, 2nd Series, 17:55-108.

Boussinesq, J., 1877. Essai sur la theorie des eaux courantes, Memoires présentés par Divers Savants a L'Acad, *Sci. Inst. France,* Series 2. 23(1):680.

Chamberlain, P.G., and Porter, D., 1995. The modified mild-slope equation, *J. Fluid Mech.*, 291: 393-407.

Chorin, A.J., 1968. Numerical solution of the Navier-Stokes equations, *Math. Comput.*, 22:745-762.

Copeland, G.J.M., 1985. A practical alternative to the mild slope wave equation, *Coastal Engrg.*, 9: 125-149.

Ebersole, B.A., Cialone, M.A., and Prater, M.D., 1986. Regional coastal processes numerical modeling system, Report 1, RCPWWAVE-A linear wave propagation model for engineering use, Technical report CERC-86-4, US Army Engineer WES, Vicksburg, Mississippi.

Isobe, M., 1994. Time-dependent mild-slope equations for random waves, *proc. 24th Int. Conf. Coastal Engrg.*, ASCE, 285-299.

Lee, J.L., 1994. Derivation of nonlinear model for irregular waves on mild slope, *J. Korea. Soc. Coast. and Ocean Eng.*, KSCOE, 6(3): 281-289.

Madsen, P.A., and Larsen, J., 1987. An efficient finite-difference approach to the mild-slope equation, *Coastal Engrg*, 11:329-351.

Madsen, P.A., Murray, R., and Sorensen, O.R., 1991. A new form of the Boussinesq equations with improved linear dispersion characteristics, *Coastal Engrg.*, 15: 371-388.

Massel, S.R., 1993. Extended refraction-diffraction equation for surface waves, *Coastal Engrg*, 19: 97-126.

McCowan, A.D., 1985. Equation systems for modeling dispersive flow in shallow water, *Proc. 21st IAHR Congr.*

Miche, R., 1951. The reflecting power of maritime works exposed to action of the waves, Annals of the Highway Dept., National Press, France.

Nadaoka, K., Beji, S., and Nakagawa, Y., 1994. A fully-dispersive weaklynonlinear wave model and its numerical solutions, *Proc. 24th Int. Conf. on Coastal Engrg.*, ASCE, 427-441.

Nadaoka, K., Beji, S., and Nakagawa, Y., 1997. A fully dispersive weakly nonlinear model for water waves, *Proc. R. Soc. Lond.* A, 453: 303-318.

Nwogu, O., 1993. An alternative form of the Boussinesq equations for nearshore wave propagation, *J. Waterway, Port, Coastal and Ocean Engrg.*, 119: 618-638.

Peregrine, D.H., 1967. Long waves on a beach, *J. Fluid Mech.*, 27(4):815-827.

Peregrine, D.H., 1974. Discussion of : A numerical simulation of the undular hydraulic jump, by M.B. Abbott and G.S. Rodenhuis., *J. Hydraul. Res.*, 12(1):141-157.

Radder, A.C., 1979. On the parabolic equation method for water-wave propagation, *J. Fluid Mech.*, 95: 159-176.

Smith, R., and Sprinks, T., 1975. Scattering of surface waves by a conical island, *J. Fluid Mech.*, 72: 373-384.

Suh, K.D., Lee, C., and Park, W.S., 1997. Time-dependent equations for wave propagation on rapidly varying topography, *Costal Engrg.*, 32:91-117.

Svendsen, I.A., 1974. Cnoidal waves over a gently sloping bottom. Tech. Univ. Denmark, Lyngby, ISVA, Ser. Pap.6.